



---

# Hemispheric and regional circulation regimes

**Franco Molteni**

European Centre for Medium-Range Weather Forecasts

*in collaboration with Susanna Corti, David Straus,  
Tim Stockdale, Frederic Vitart*



# Outline

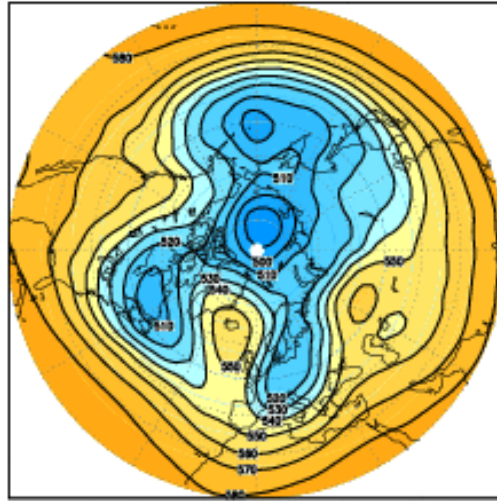
---

- Introduction: Historical overview on regime theory and modelling
- Detection of regimes in atmospheric and model datasets
- A new look at “hemispheric” and regional regimes using ERA-Interim data
- How to interpret the impact of anomalies in tropical “forcing”

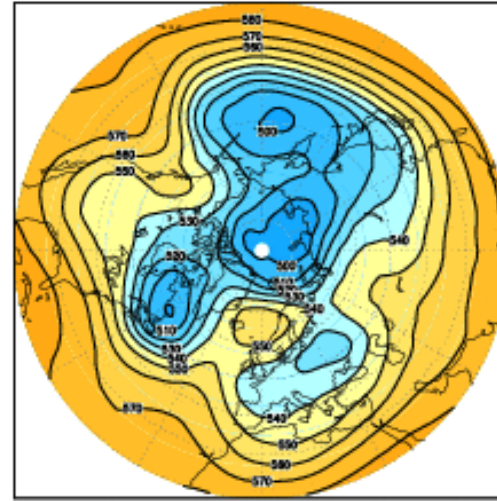


# Recurrent flow patterns: examples

5-9 Jan  
1985

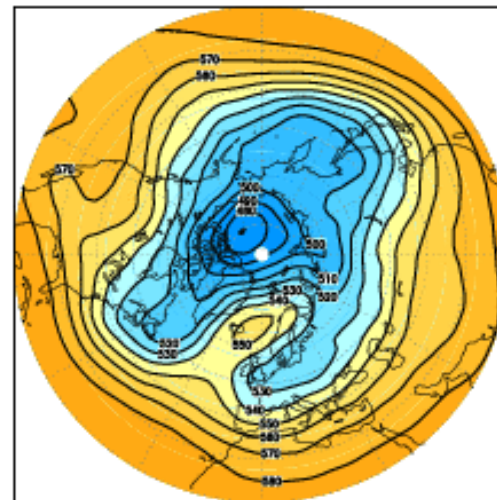


4-8 Feb  
1986



A selection of 5-day mean  
fields of 500 hPa  
geopotential height  
during boreal winter ...

10-14 Jan  
1987



# Regimes as quasi-stationary states

---

$q$  : barotropic or quasi-geostrophic potential vorticity

$$\partial_t q = - V_\psi \cdot \textit{grad} q - D (q - q^*)$$

steady state for instantaneous flow:

$$0 = - V_\psi \cdot \textit{grad} q - D (q - q^*)$$

steady state for time-averaged flow:

$$0 = - \langle V_\psi \rangle \cdot \textit{grad} \langle q \rangle - D (\langle q \rangle - q^*) \\ - \langle V'_\psi \cdot \textit{grad} q' \rangle$$



# Charney and DeVore 1979

Multiple steady states of low-order barotropic model with wave-shaped bottom topography

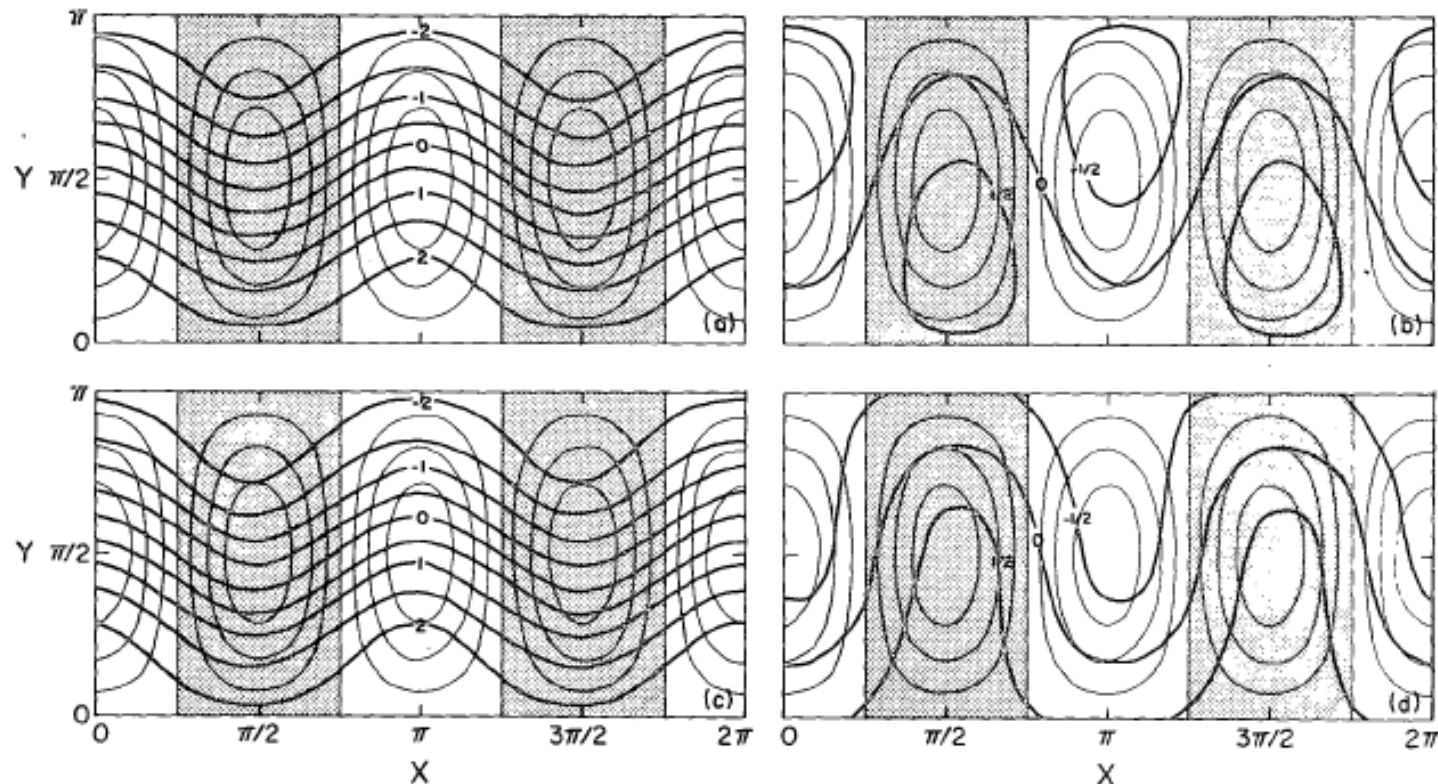


FIG. 4. Streamfunction fields of the stable first mode equilibria of a topographically forced flow for  $k = 10^{-2}$ ,  $L/a = 1/4$ ,  $n = 2$ ,  $h_0/H = 0.2$  and  $\psi_0^* = 0.2$ : for the spectral model above resonance (a) and slightly below resonance (b); and for the grid-point model above resonance (c) and slightly below resonance (d). The nondimensional topographic heights are shown with light lines; the contour spacing is 0.05 units, with negative regions shaded.

## Papers on multiple equilibria and quasi-stationary states

---

### Orographically forced models:

- **Charney and Straus 1980:** *Form-grad instability, multiple equilibria and propagating planetary waves in baroclinic, orographically-forced planetary wave systems*
- **Charney, Shukla and Mo 1981:** *Comparison of barotropic blocking theory with observation*
- **Legras and Ghil 1985:** *Persistent anomalies, blocking and variations in atmospheric predictability*
- **Benzi, Malguzzi, Speranza, Sutera 1986:** *The statistical properties of the atmospheric general circulation: observational evidence and a minimal theory of bimodality*

### Thermally forced models:

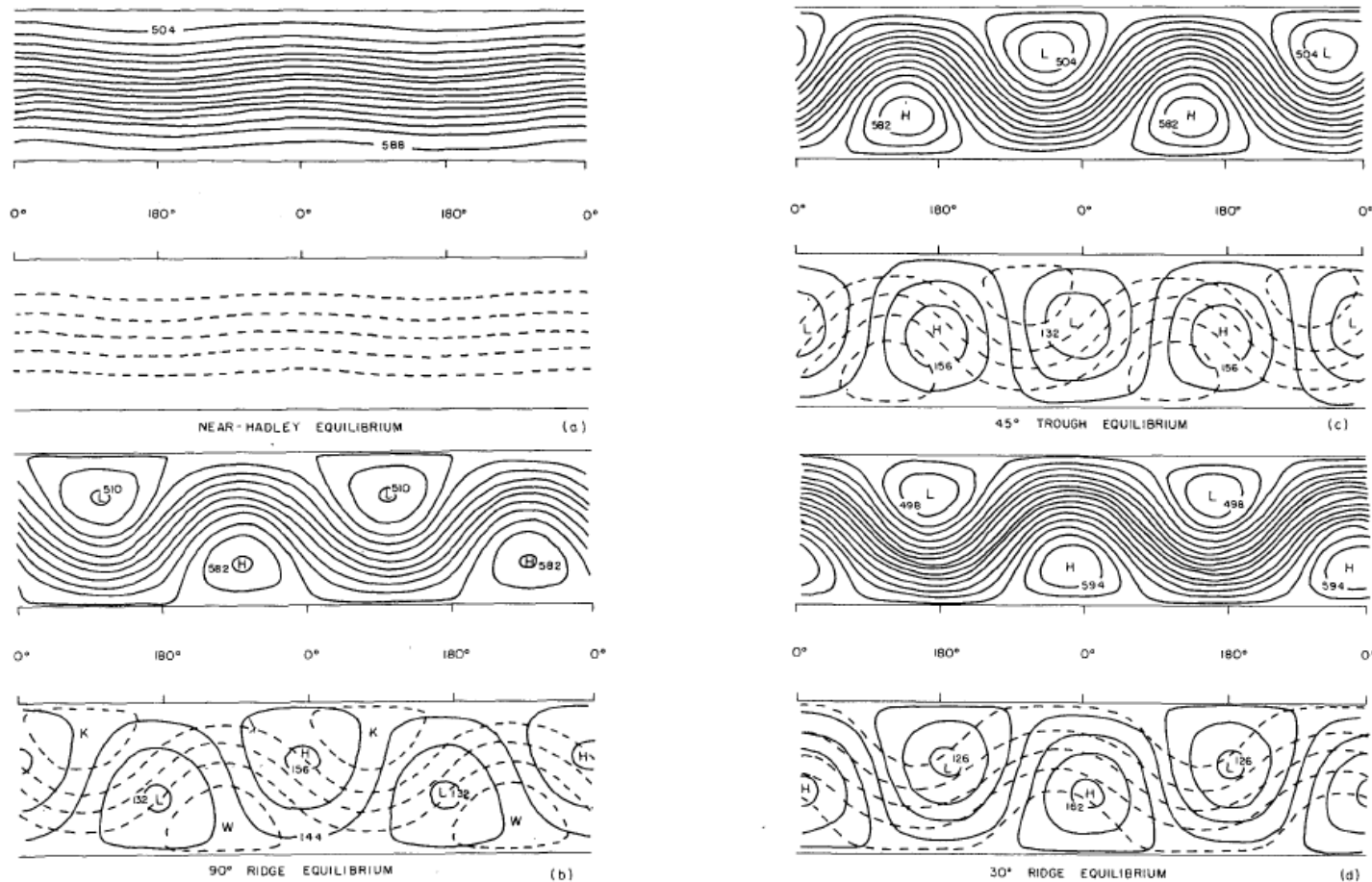
- **Mitchell and Derome 1983:** *Blocking-like solutions of the potential vorticity equation: their stability at equilibrium and growth at resonance*





# Reinhold and Pierrehumbert 1983

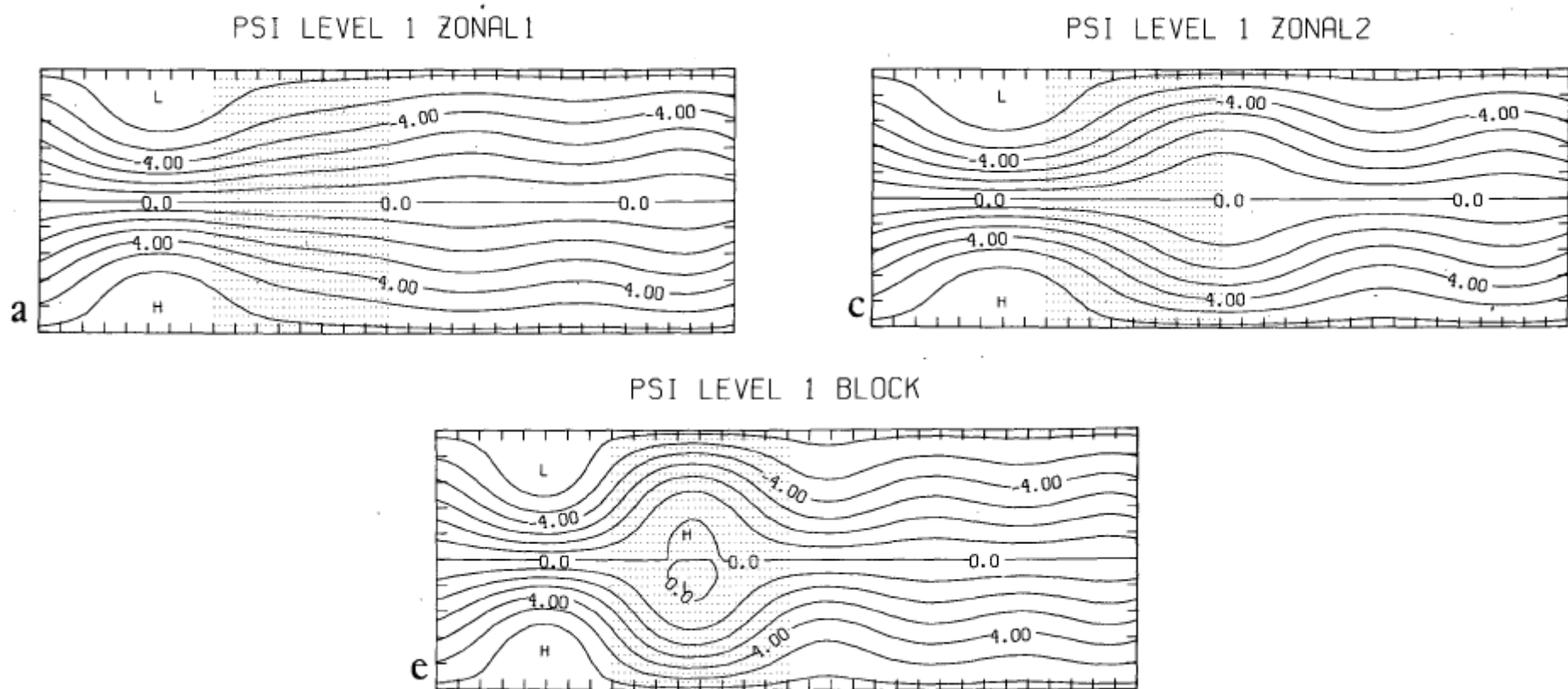
Hemispheric weather regimes arising from equilibration of large-scale dynamical tendencies and "forcing" from transient baroclinic eddies





# Vautard and Legras 1988

Regional weather regimes arising from equilibration of large-scale dynamical tendencies and PV fluxes from transient baroclinic eddies







# Looking for bimodality: Hansen and Sutera 1986

Bimodality in the probability density function (PDF) of an index of N. Hem. planetary wave amplitude due to near-resonant wave-numbers ( $m=2-4$ )

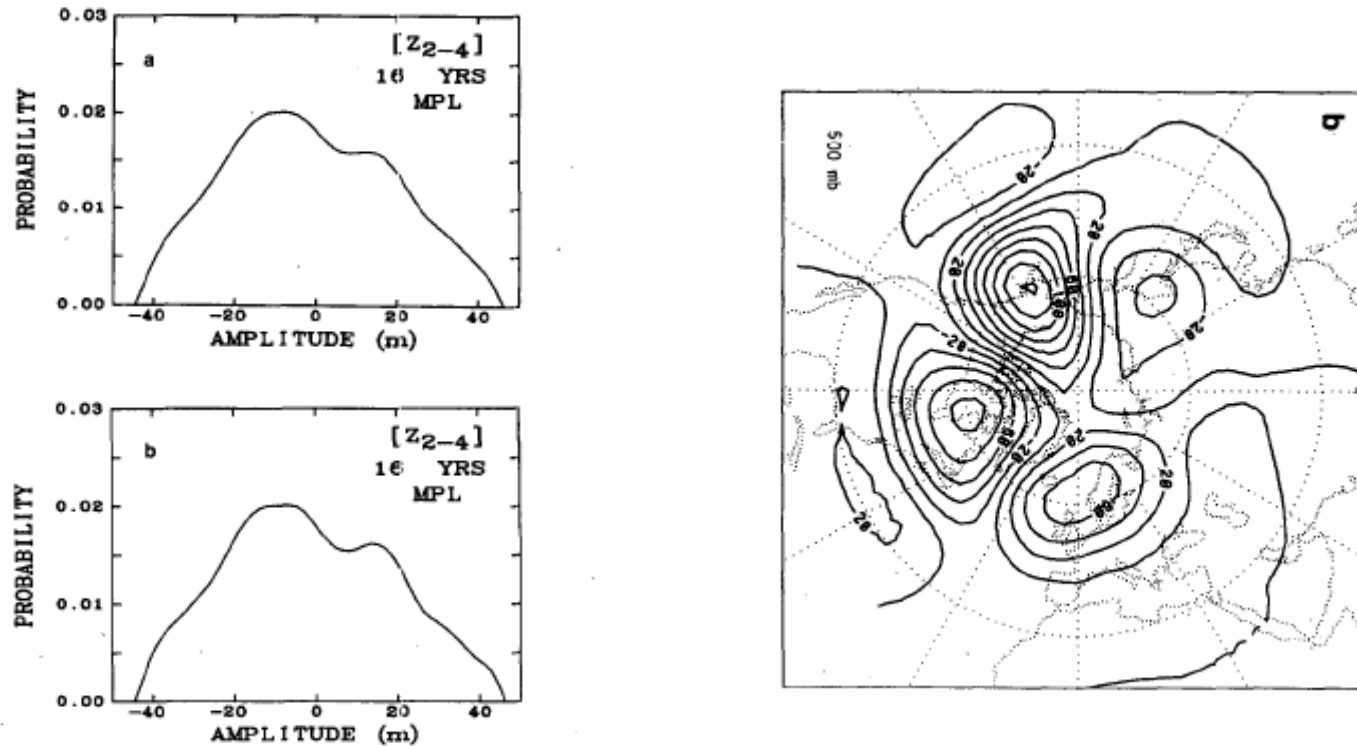


FIG. 4. MPL probability density estimates of  $[Z_{2-4}]$  formed from the 16 winter composite filtered data for (a)  $\alpha = 10^7$  and (b)  $\alpha = 5 \times 10^6$ .

# Multi-dim. PDF estimation and cluster analysis

Searching for densely-populated regions in phase space:

- Mo and Ghil 1988
- Molteni et al. 1990
- Cheng and Wallace 1993
- Kimoto and Ghil 1993a, b
- Michelangeli et al. 1995
- Corti et al. 1999

Kimoto and Ghil 1993a →

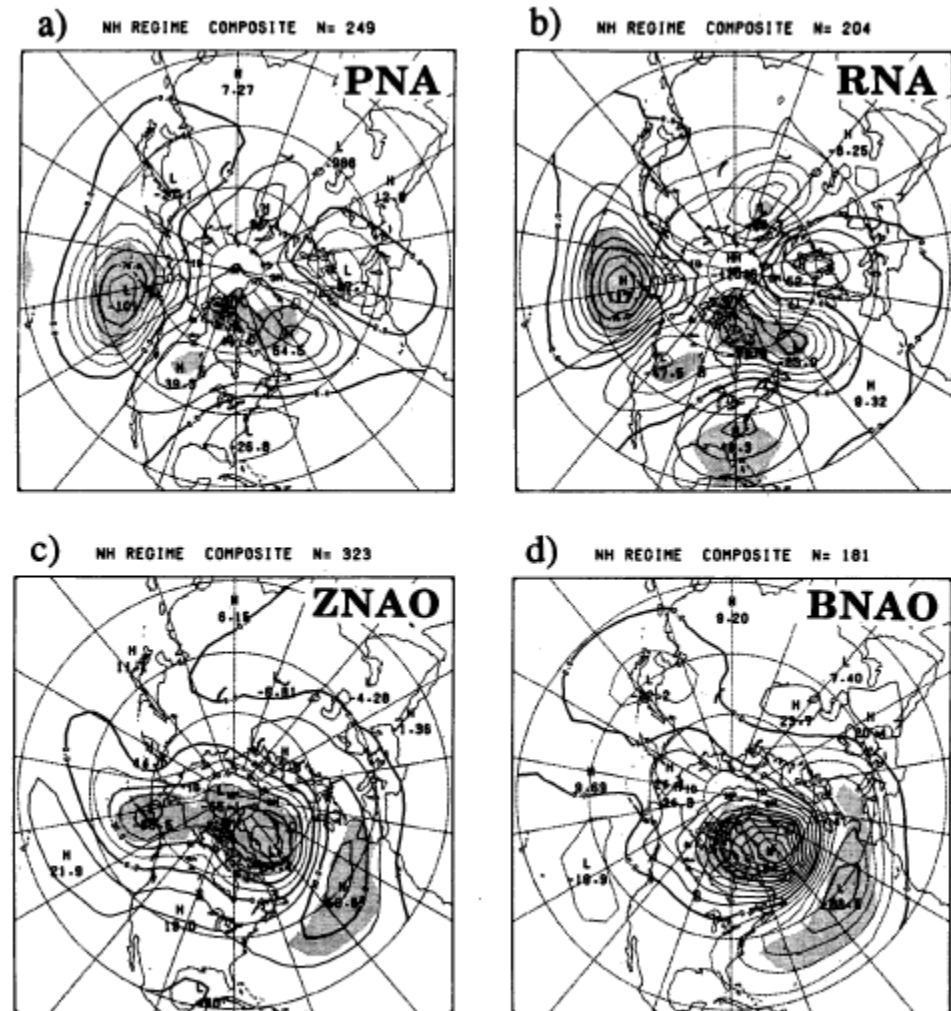


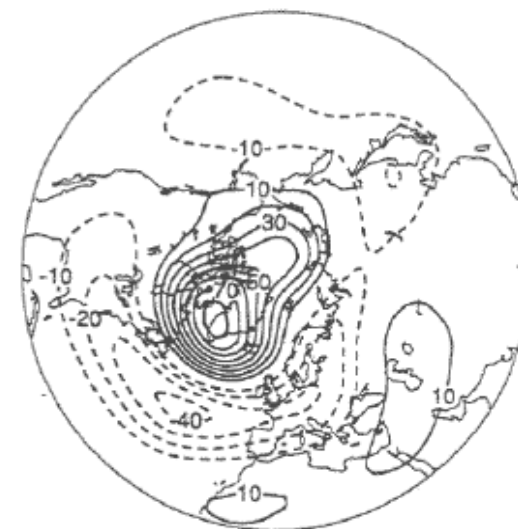
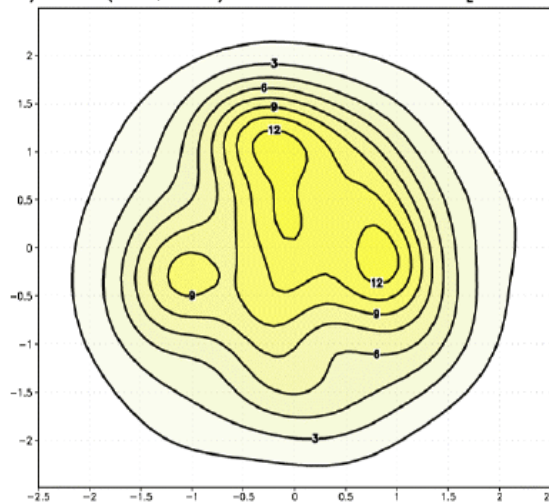
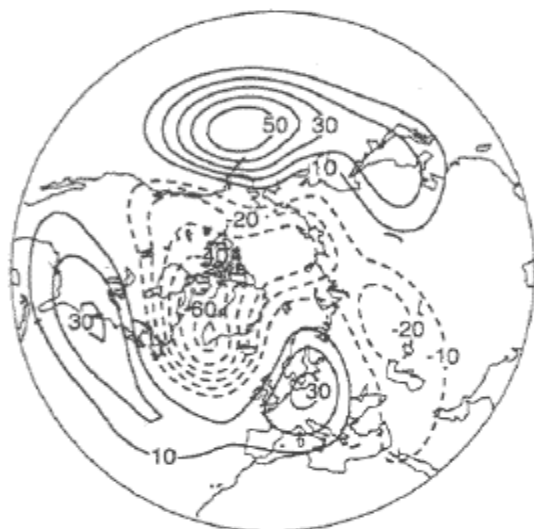
FIG. 14. Composite maps of unfiltered anomalies for the four NH regimes. Those samples falling in either of the four rectangles in Fig. 11a are collected for (a) PNA, (b) RNA, (c) ZNAO, and (d) BNAO. Numbers of collected daily maps are (a) 249, (b) 204, (c) 323, and (d) 181, respectively. Contour interval is 15 meters; shaded regions are significantly different from zero at a 99% level judged by a pointwise *t*-test.



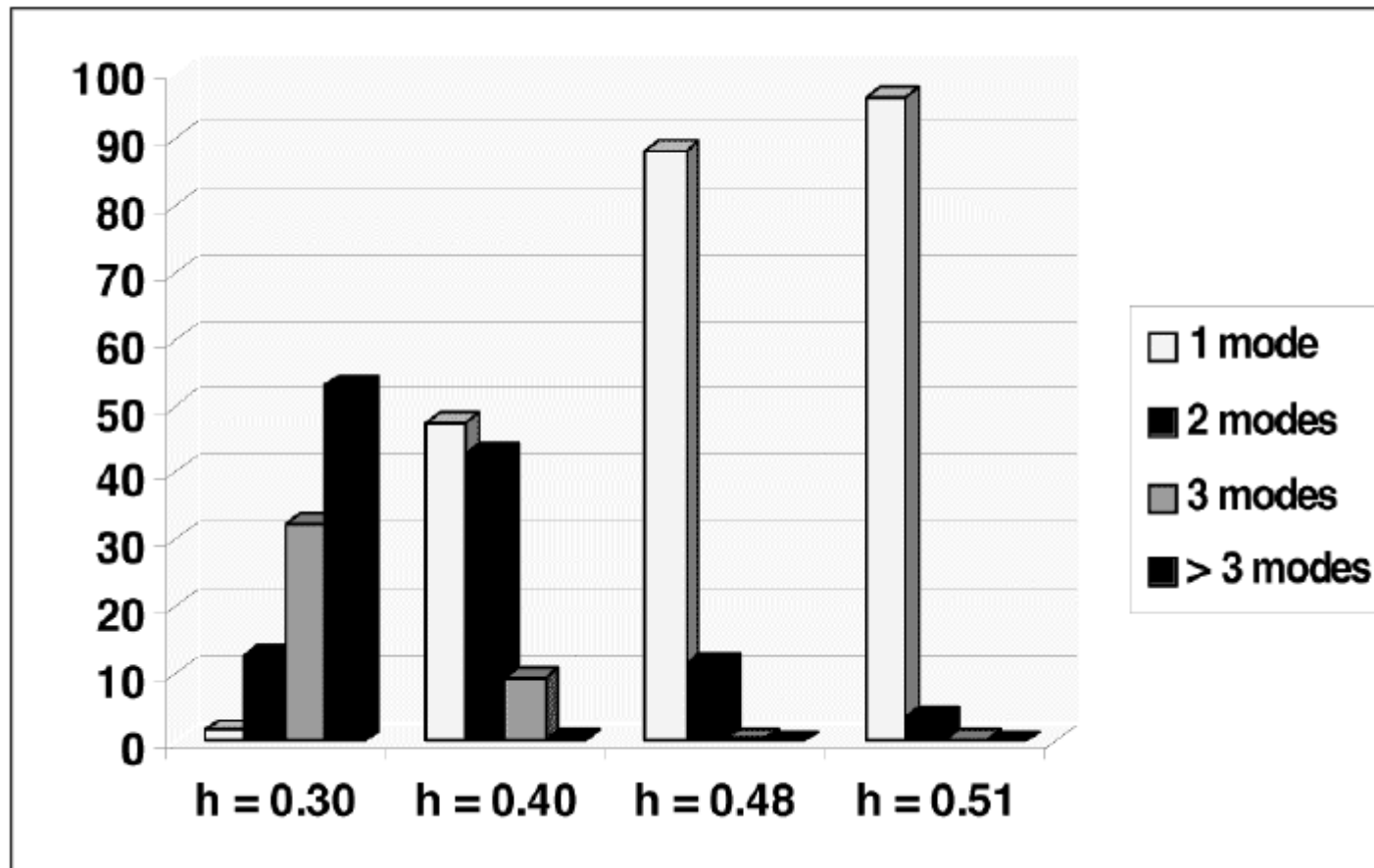
# Regimes from PDF estimation (Corti et al. 1999)



b) PDF (PC1, PC2) Re-An. 1955-98 [h = 0.4]



# PDF estimation: statistical significance



Fraction of uni/multi-modal PDFs obtained from a gaussian distribution  
sample size as in Corti et al. 1999

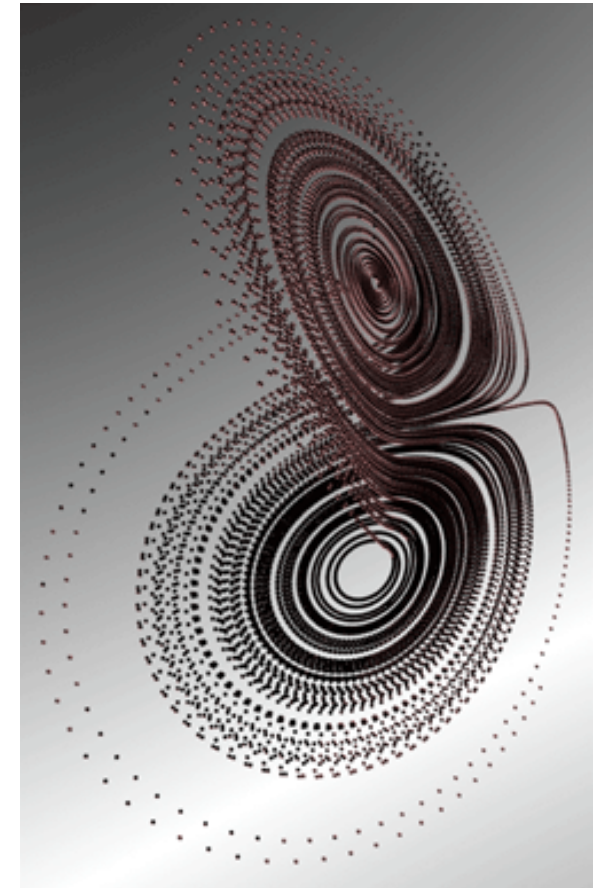
# ↻ Impact of external forcing in non-linear systems

*Lorenz (1963) truncated convection model with additional forcing  $f$  (Molteni et al. 1993; Palmer 1993)*

- $dX/dt = \sigma (Y - X)$
- $dY/dt = -XZ + rX - Y + f$
- $dZ/dt = XY - bZ$

***Unstable stationary states (for  $f=0$ )***

- $X = Y = Z = 0$
- $X = Y = \pm [b(r-1)]^{1/2}, Z = r-1$



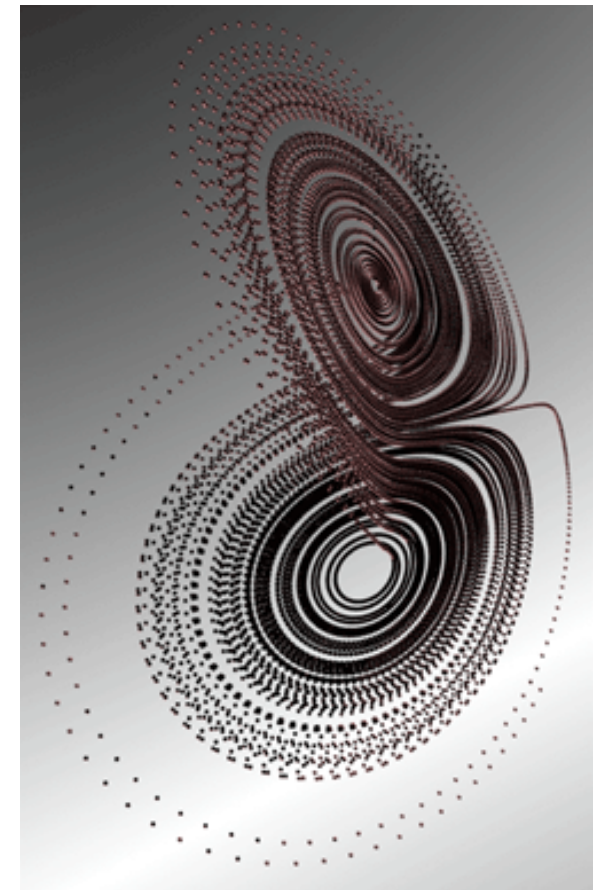


# ↻ Impact of external forcing in non-linear systems

---

The properties of atmospheric flow regimes may be affected by anomalies in boundary forcing in different ways:

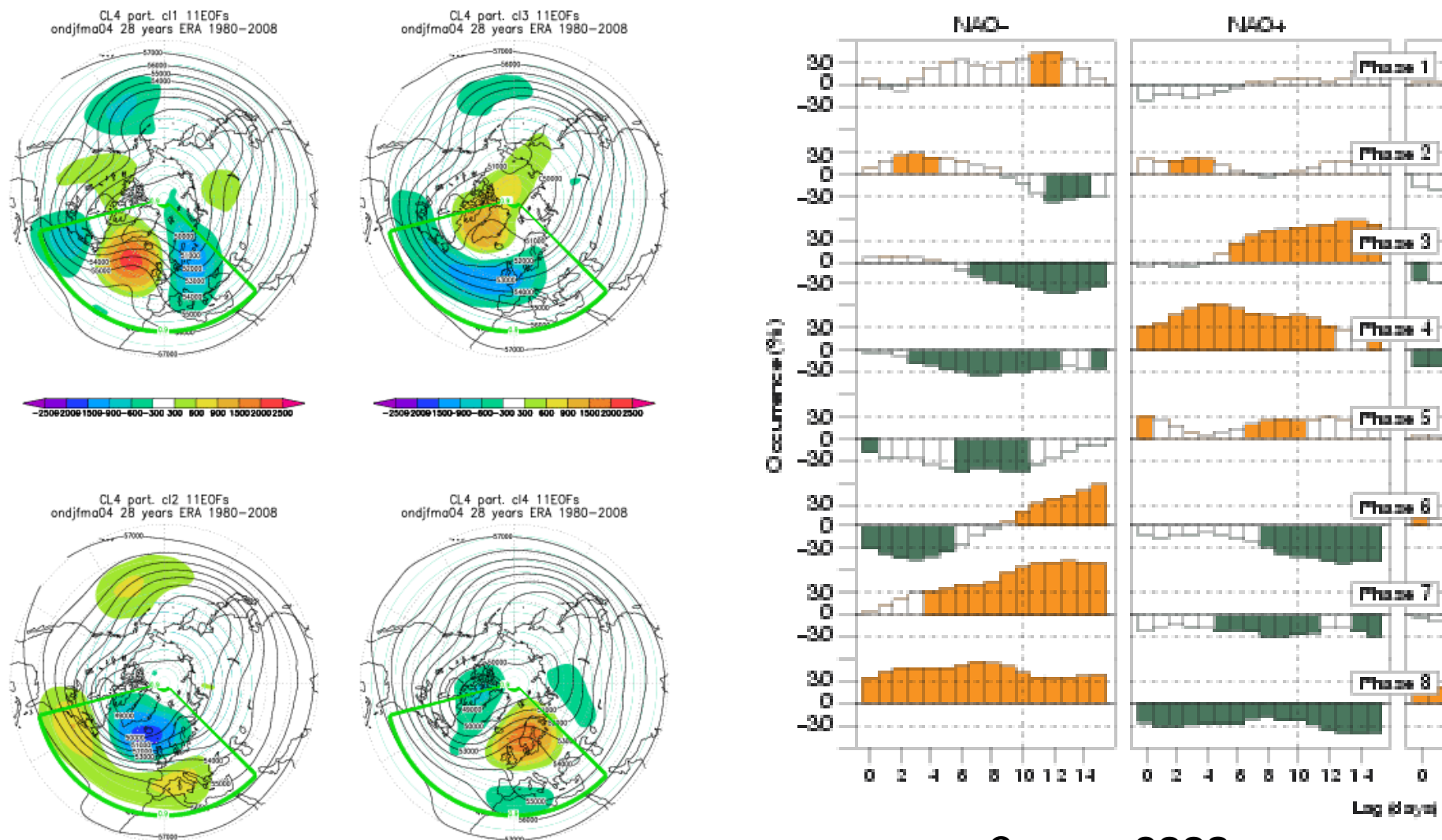
- **Weak forcing anomaly:** the number and spatial patterns of regimes remain the same, but their frequency of occurrence is changed (“Lorenz model paradigm”)
- **Strong forcing anomaly:** the number and patterns of regimes are modified as the atmospheric system goes through bifurcation points







# Euro-Atlantic regimes and the impact of MJO



Cassou 2008



# Pacific – North American regimes

Cluster analysis of low-freq. ( $T > 10$  d) Z 200 in NCEP re-analysis and COLA AGCM ensembles (Straus, Corti, Molteni 2007)

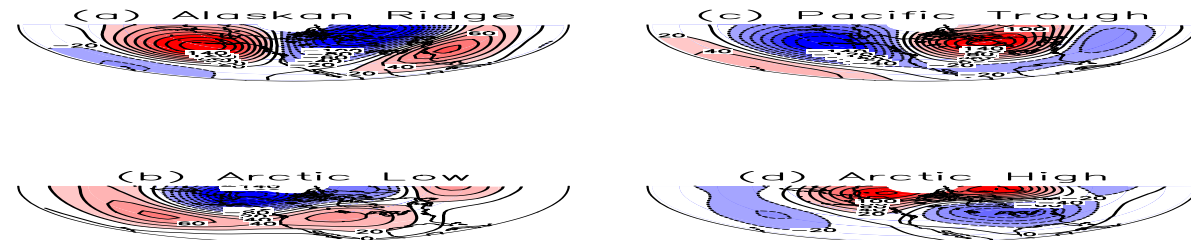


Figure 2: Cluster centroid maps of 200 hPa height for  $k = 4$  from the NCEP18 record. The cluster analysis was carried out using 6 ICFs and a value of  $\alpha = 0.5$  (see text for explanation). Contour interval is 20m, with the 0 contour omitted.

45

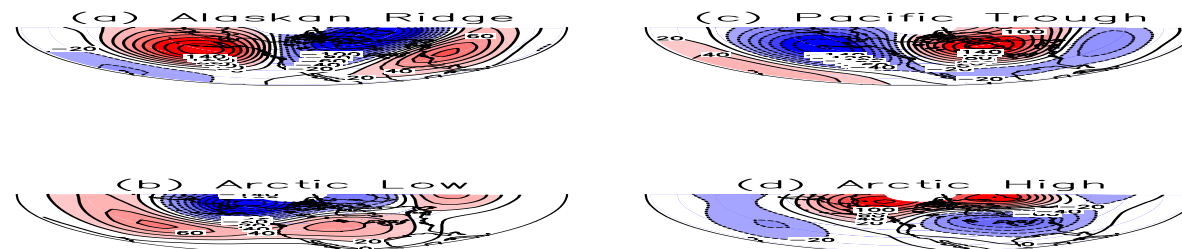


Figure 2: Cluster centroid maps of 200 hPa height for  $k = 4$  from the NCEP18 record. The cluster analysis was carried out using 6 ICFs and a value of  $\alpha = 0.5$  (see text for explanation). Contour interval is 20m, with the 0 contour omitted.

45



# Does ENSO affect the number of regimes?

- Ratio of inter-cluster to intra-cluster variance as a function of ENSO indices (Straus and Molteni 2004)

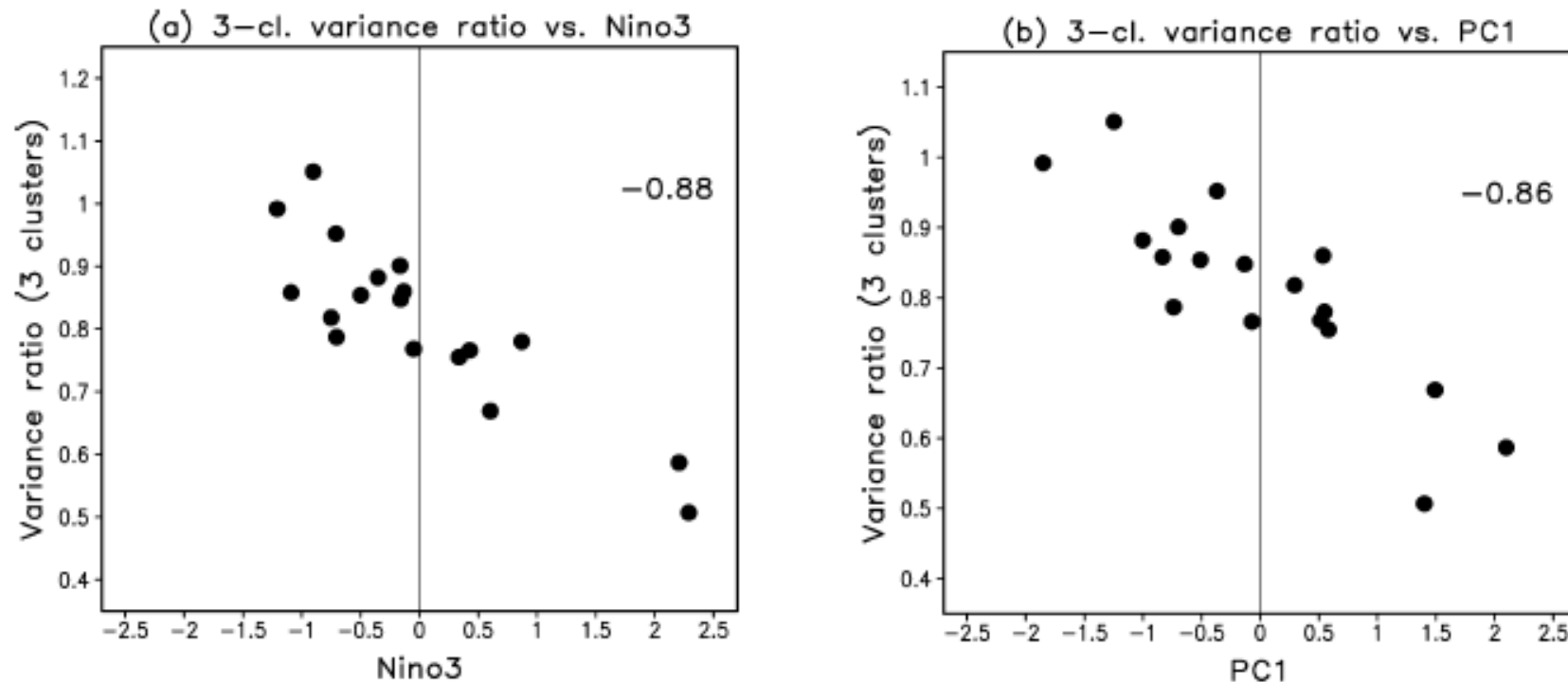


FIG. 4. Scatterplots of (a) the 3-cluster ( $k = 3$ ) variance ratio vs Niño-3, and (b) the 3-cluster variance ratio vs the leading PC of ensemble/seasonal means. The leading PC and SST index time series are standardized.

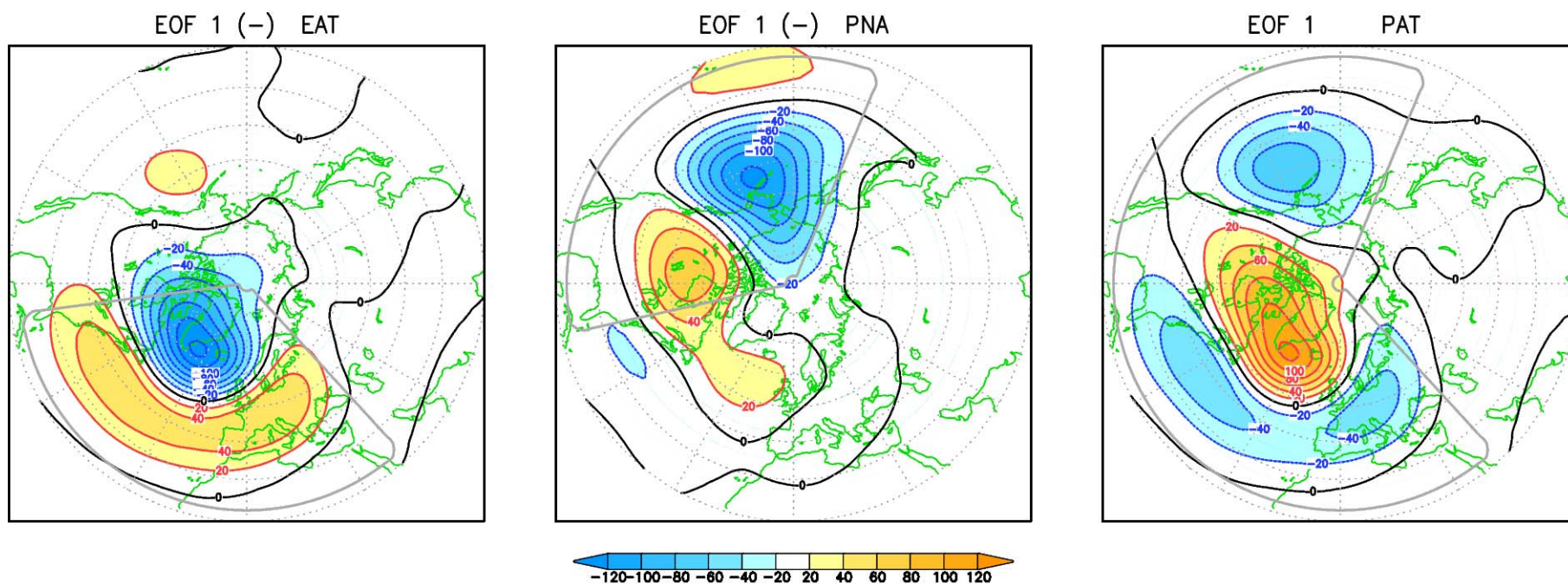
# A re-visitation of Pacific + Atlantic regimes: methodology

---

- **Data:**
  - 5-day means of 500-hPa height from ERA-Interim
  - Dec.1979-Mar.1980 to Dec.2012-Mar.2013 (24 pentads\*34 years = 816)
- **Definition of anomalies wrt 34-yr climate (low-pass filtered)**
- **EOF analysis on 3 domains:**
  - Euro-Atlantic (EAT: 80W-40E, 25-85N)
  - Pacific – North America (PNA: 160E-80W, 25-85N)
  - Pacific + Atlantic (PAT = PNA + EAT, 160E-40E, 25-85N)
- **Non-hierarchical cluster analysis using k-means algorithm**
  - up to 6 clusters for EAT and PNA, up to 8 clusters for PAT
  - Significance test on signal-to-noise ratio (centroid variance / inter-cluster variance) against 500 red-noise data samples with same variance, skewness and lag-1 autocorrelation as individual PCs)
  - Refs.: Michelangeli et al. 1995, Straus et al. 2007

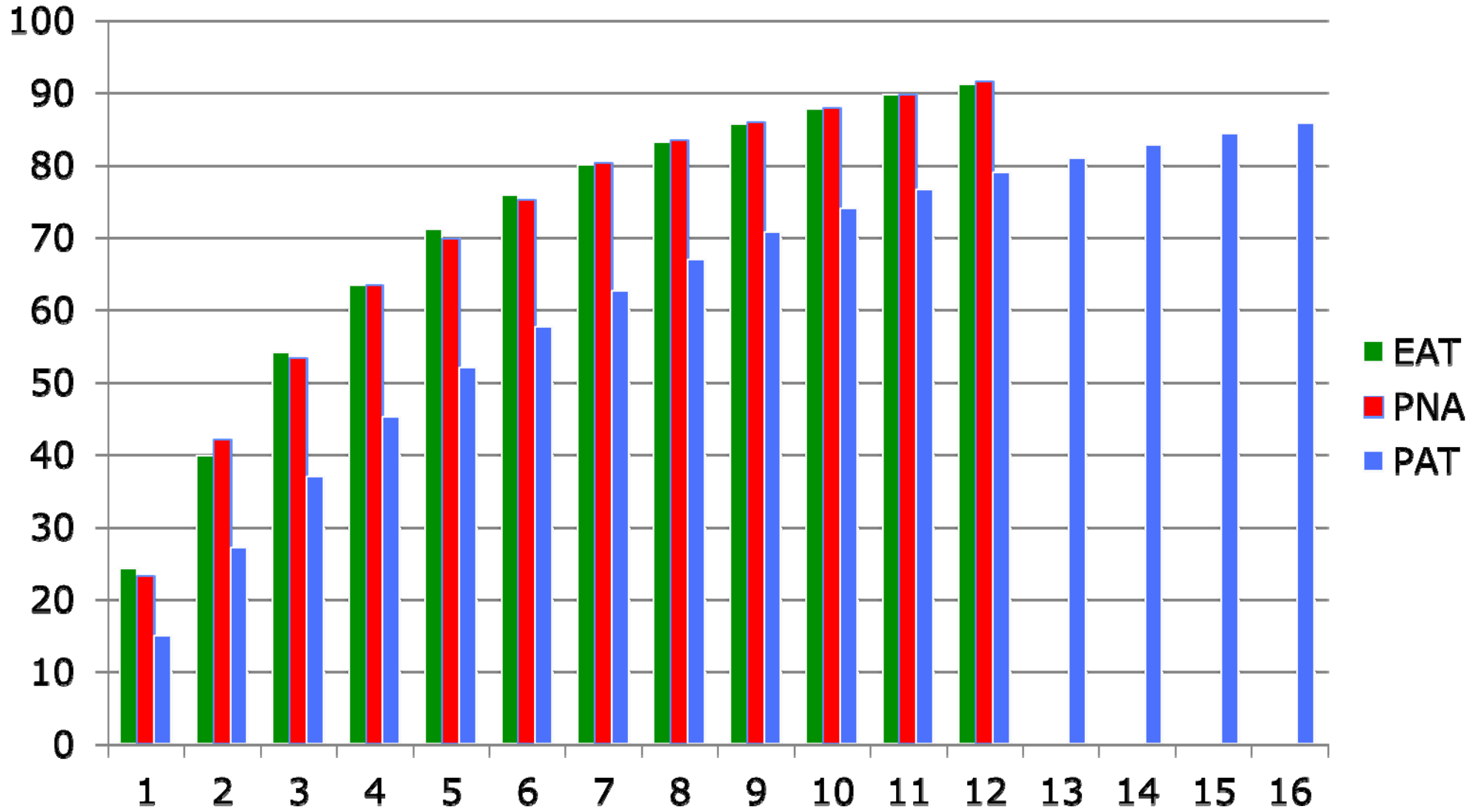


# EOF-1 for the three domains





# variance of N EOFs (%) in the three domains







# S/N variance ratio and multi-modality

## a) 2 regimes in 1 dimension:

$$P(x) = 0.5 [ G(\mu, \sigma) + G(-\mu, \sigma) ]$$

$$\text{Total variance} = \mu^2 + \sigma^2$$

$$\text{S/N variance ratio} = \mu^2 / \sigma^2$$

$P(x)$  is bimodal if  $S/N > 1$

$$\mu = 0.8, \quad \sigma_x = 0.6: \quad \text{S/N} = 1.78$$

$$\mu = 0.71, \quad \sigma_x = 0.71: \quad \text{S/N} = 1.00$$

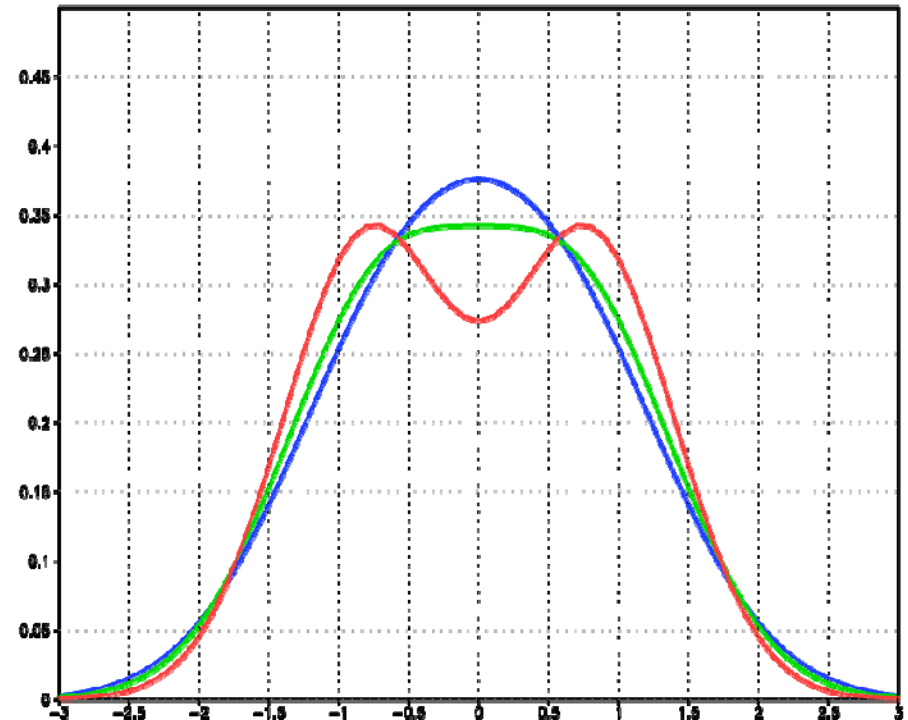
$$\mu = 0.6, \quad \sigma_x = 0.8: \quad \text{S/N} = 0.56$$

## b) 2 regimes in 2 dimensions

$$P(x, y) = P(x) P(y)$$

$$P(x) = 0.5 [ G(\mu, \sigma_x) + G(-\mu, \sigma_x) ], \quad P(y) = G(0, \sigma_y)$$

$$\text{If } \mu = \sigma_x = \sigma_y = 0.71: \quad \text{S/N} = \mu^2 / (\sigma_x^2 + \sigma_y^2) = 0.5$$



**For N regimes, S/N should be  $> 1$  in a subspace of N-1 dimensions**  
(a lower limit applies to regimes with different population)



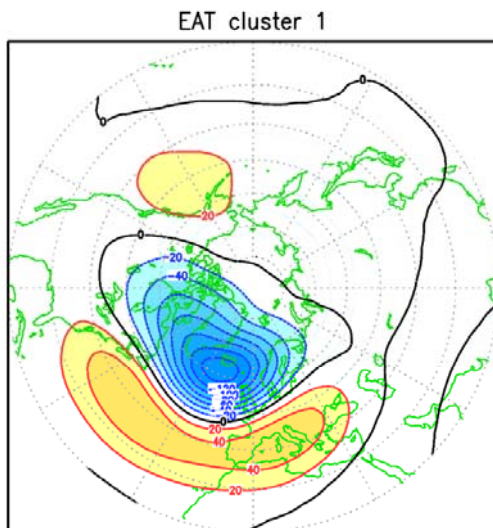
## Statistics for N-cluster partitions (%)

	2 cl	3 cl	4 cl	5 cl	6 cl	7 cl	8cl
<b>E-AT var s/n</b>	24.7	42.3	59.3 (51.2)	71.4	81.5		
<b>E-AT conf.lev</b>	52.7	86.8	<b>99.8</b>	99.6	99.8		
<b>P-NA var s/n</b>	24.2	43.8	57.9 (49.7)	69.4	79.1		
<b>P-NA conf.lev</b>	76.0	87.6	<b>98.6</b>	98.8	99.0		
<b>P-AT var s/n</b>	15.6	27.3	36.3	43.6	50.0 (54.2)	55.7	61.2
<b>P-AT conf.lev</b>	57.0	76.2	90.4	93.0	<b>97.4</b>	98.0	98.8

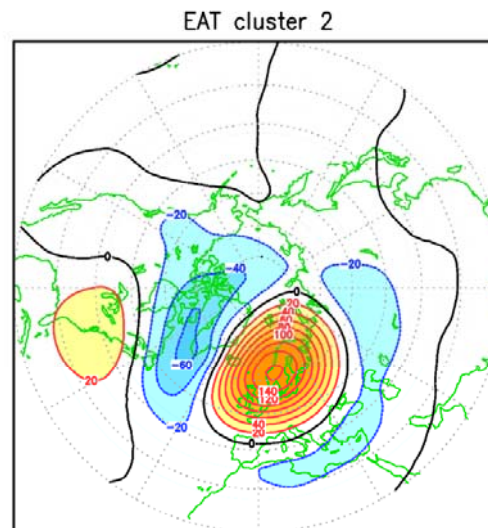


# Euro-Atlantic 4-cluster centroids

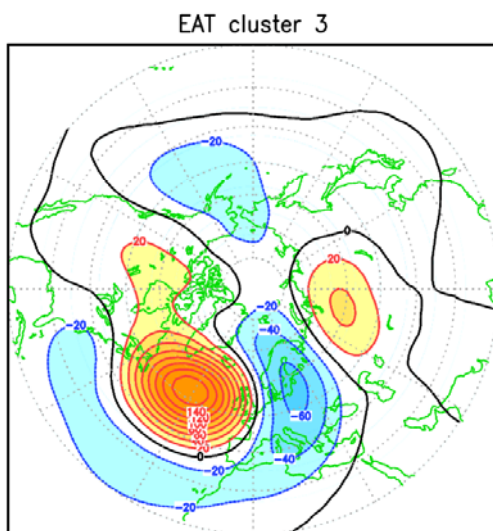
**NAO+**  
**31.5%**



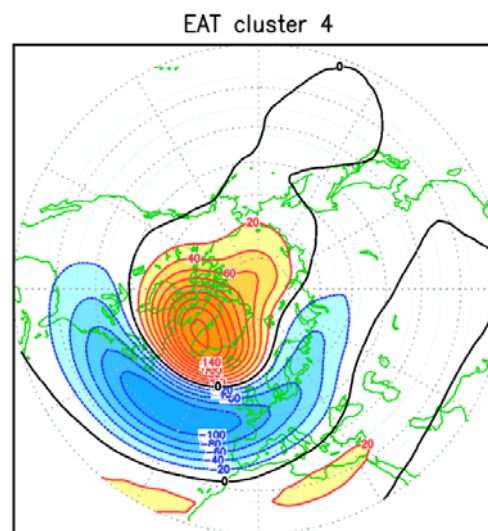
**Blocking**  
**25.0%**



**Atl. Ridge**  
**22.2%**



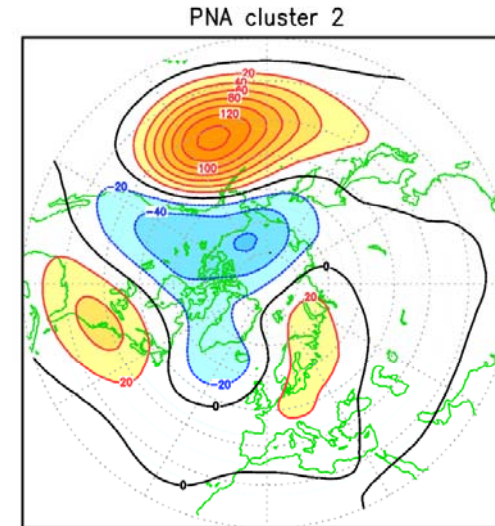
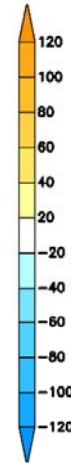
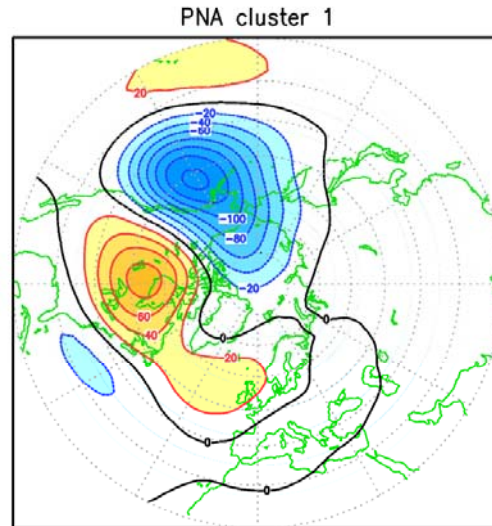
**NAO-**  
**21.3%**





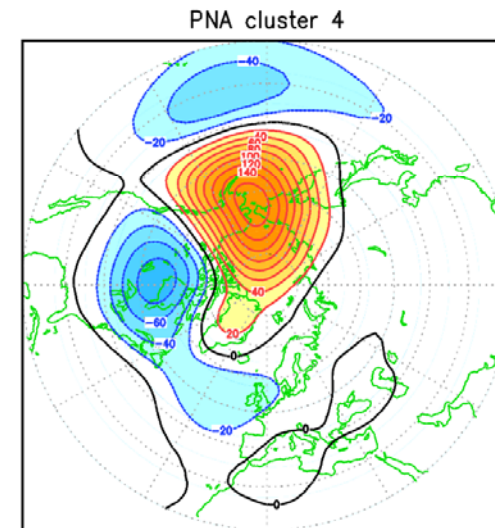
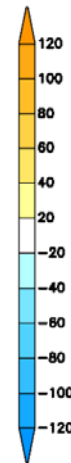
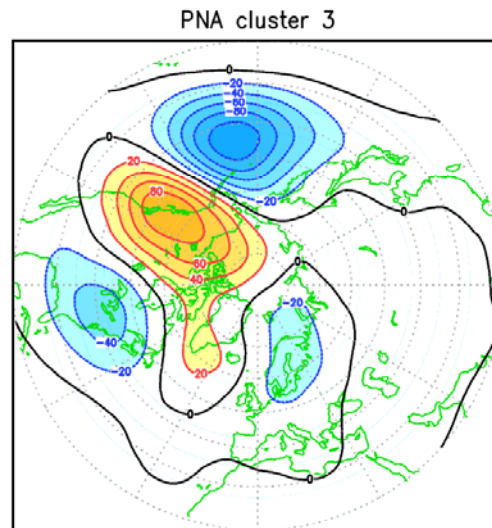
# Pacific-North American 4-cluster centroids

**Pacific  
Trough  
27.7%**



**Arctic  
Low  
27.7%**

**PNA+  
24.0%**



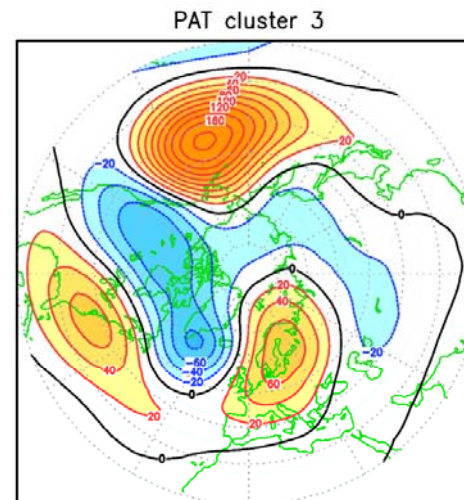
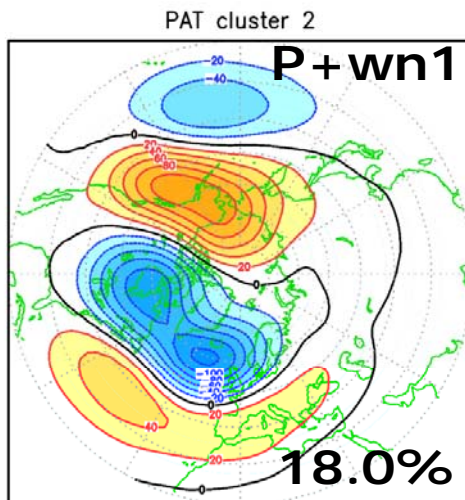
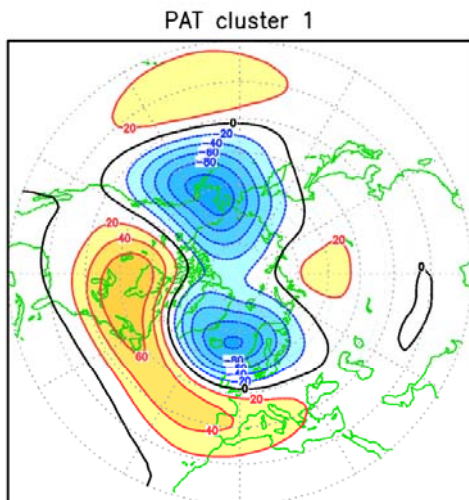
**Alaskan  
Ridge  
20.6%**





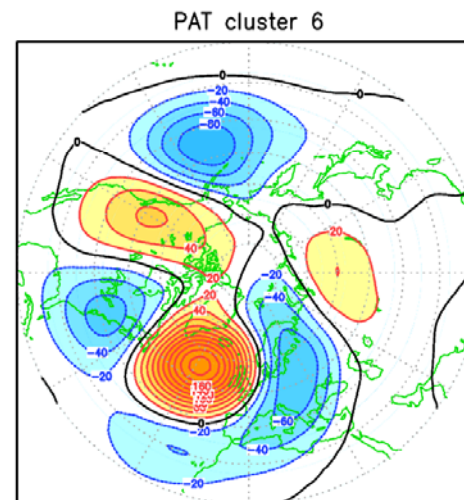
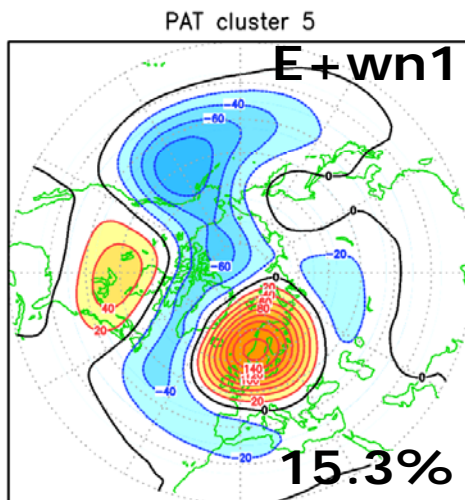
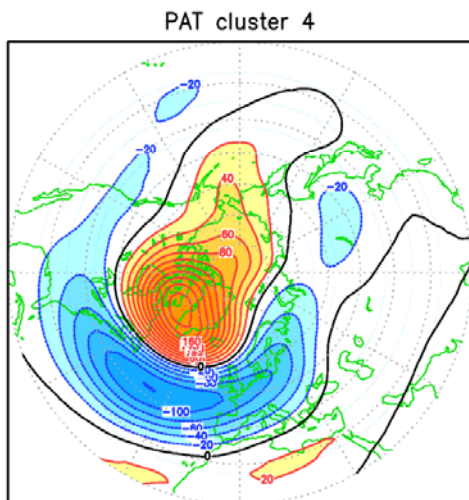
# Pacific+Atlantic 6-cluster centroids

**COWL**  
**18.8%**



**P+wn3**  
**17.6%**

**NAO-**  
**16.5%**



**A+wn3**  
**13.7%**



## Confidence levels for PAT clusters (%)

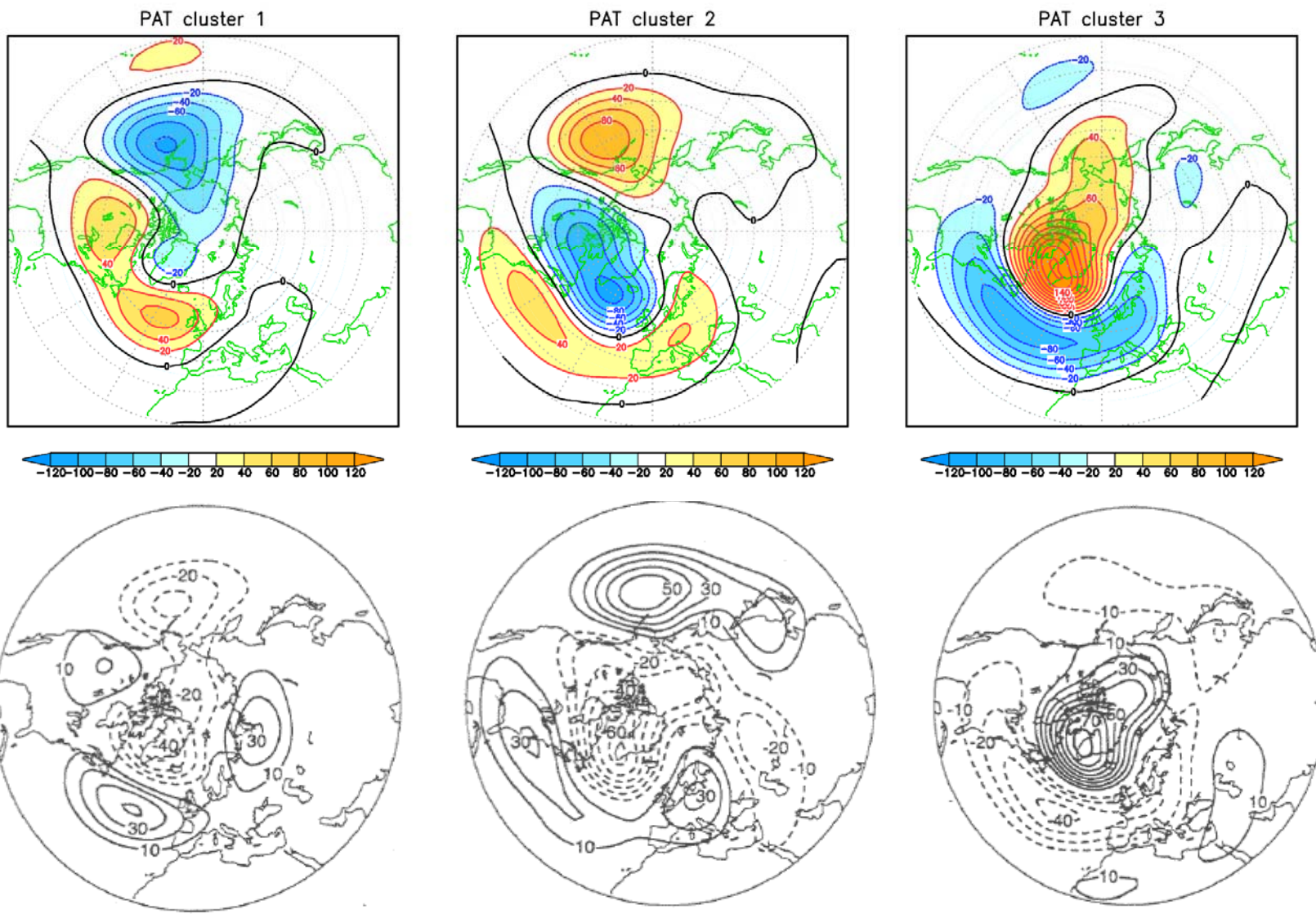
	2 cl	3 cl	4 cl	5 cl	6 cl	7 cl	8 cl
Res = 0 Skw = 0	66.6	<b>96.0</b>	100.	99.8	100.	100.	100.
Res = 0 Skw = 1	67.4	91.0	<b>99.6</b>	100.	100.	100.	100.
Res = 1 Skw = 0	57.2	79.2	92.8	<b>95.6</b>	98.6	98.6	99.0
Res = 1 Skw = 1	57.0	76.2	90.4	93.0	<b>97.4</b>	98.0	98.8

Red-noise data : prescribed mean=0, s.dev. and lag-1 autocor. as PC  
Res = 1: re-sampling from larger samples (10x)  
Skw = 1: prescribed skewness from PC samples





# P-AT 3 clusters vs. PDF modes of Corti et al. (1999)



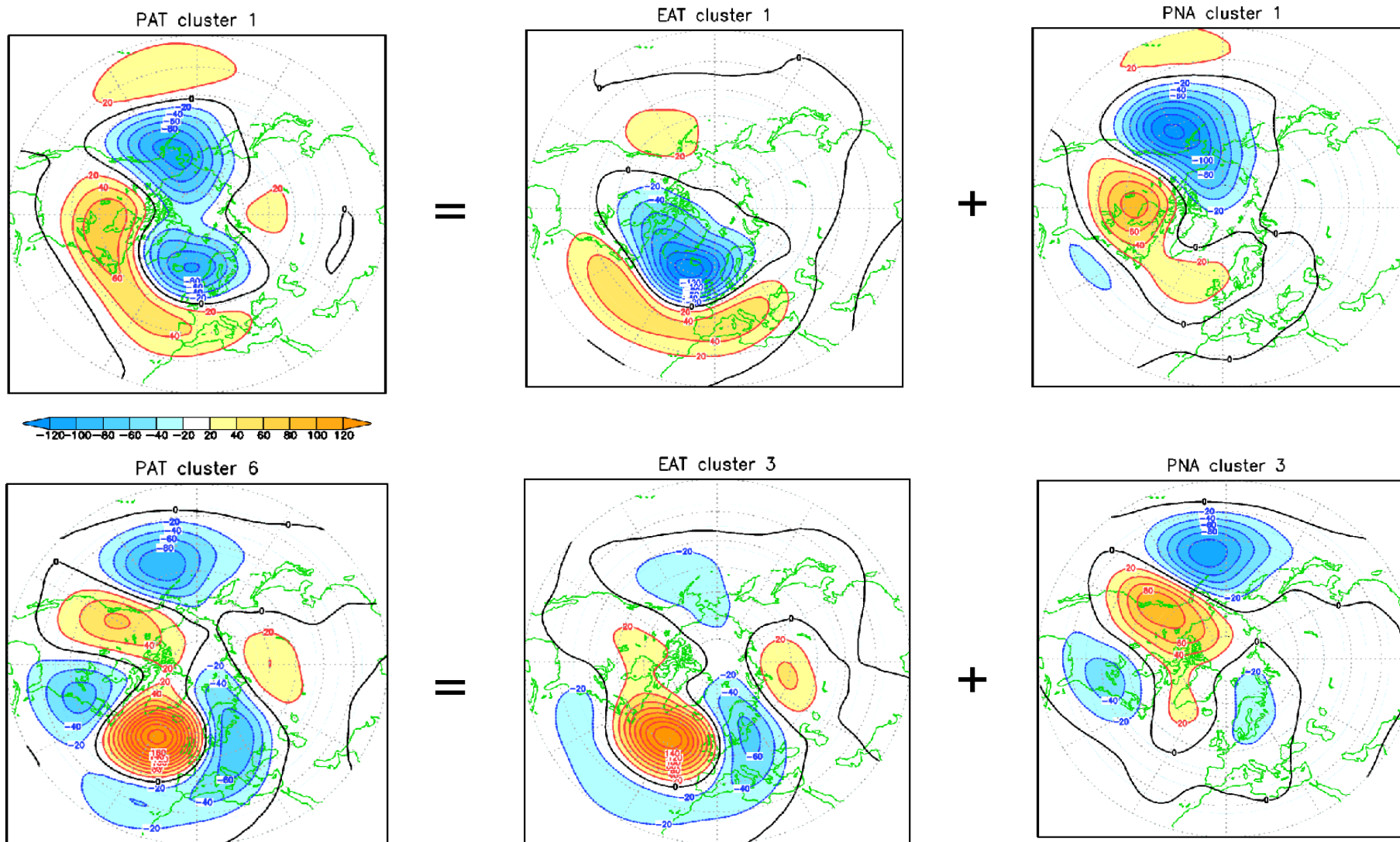


# Partition of PAT cluster frequencies into regional regimes

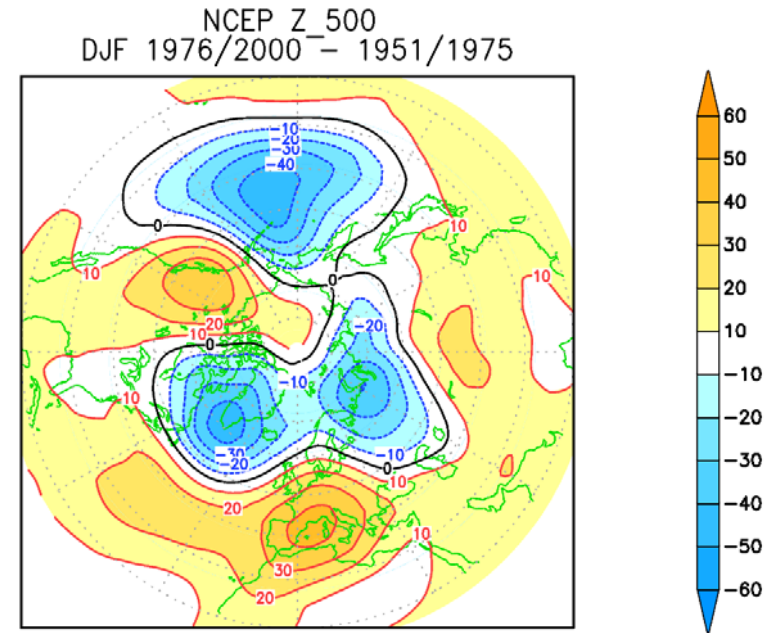
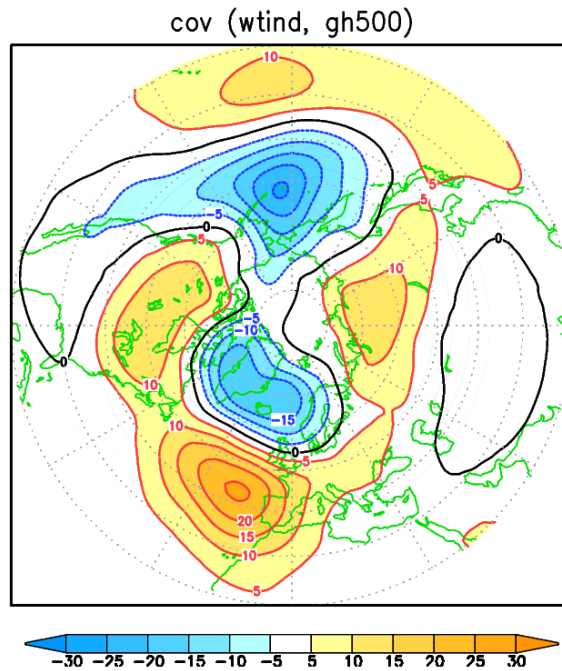
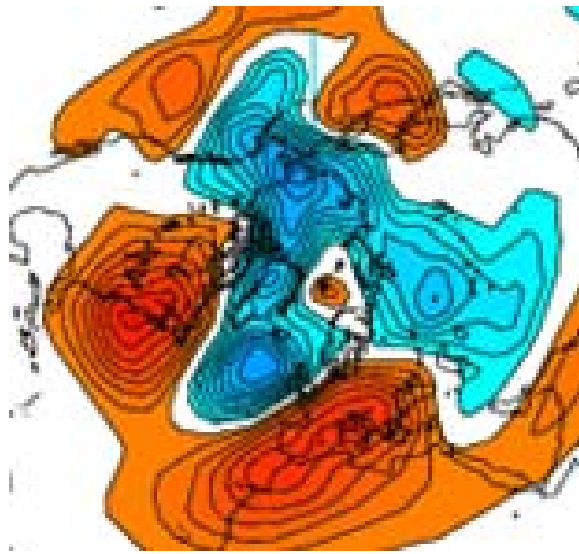
	E-AT 1 NAO+	E-AT 2 Bloc	E-AT 3 Atl-R	E-AT 4 NAO-	P-NA 1 Pac-T	P-NA 2 Arc-L	P-NA 3 PNA+	P-NA 4 Aik-R
PAT 1 COWL	<u>10.05</u>	1.23	6.25	1.23	<b>12.38</b>	4.41	1.84	0.12
PAT 2 P+wn1	<b>13.73</b>	2.21	0.98	1.10	0.25	1.84	6.25	<u>9.68</u>
PAT 3 P+wn3	6.50	<u>8.33</u>	1.96	0.96	0	<b>14.58</b>	0	3.06
PAT 4 NAO-	0.25	0.12	0.86	<b>15.32</b>	2.33	2.94	<b>5.88</b>	5.39
PAT 5 E+wn1	0.98	<b>12.13</b>	0.74	1.47	<b>9.19</b>	2.21	3.19	0.74
PAT 6 A+wn3	0	0.98	<b>11.40</b>	1.35	<b>3.55</b>	1.72	<u>6.86</u>	1.59



# Examples of regime combinations



# A planetary-wave signal common to different time scales?



## Z 500hPa anomaly

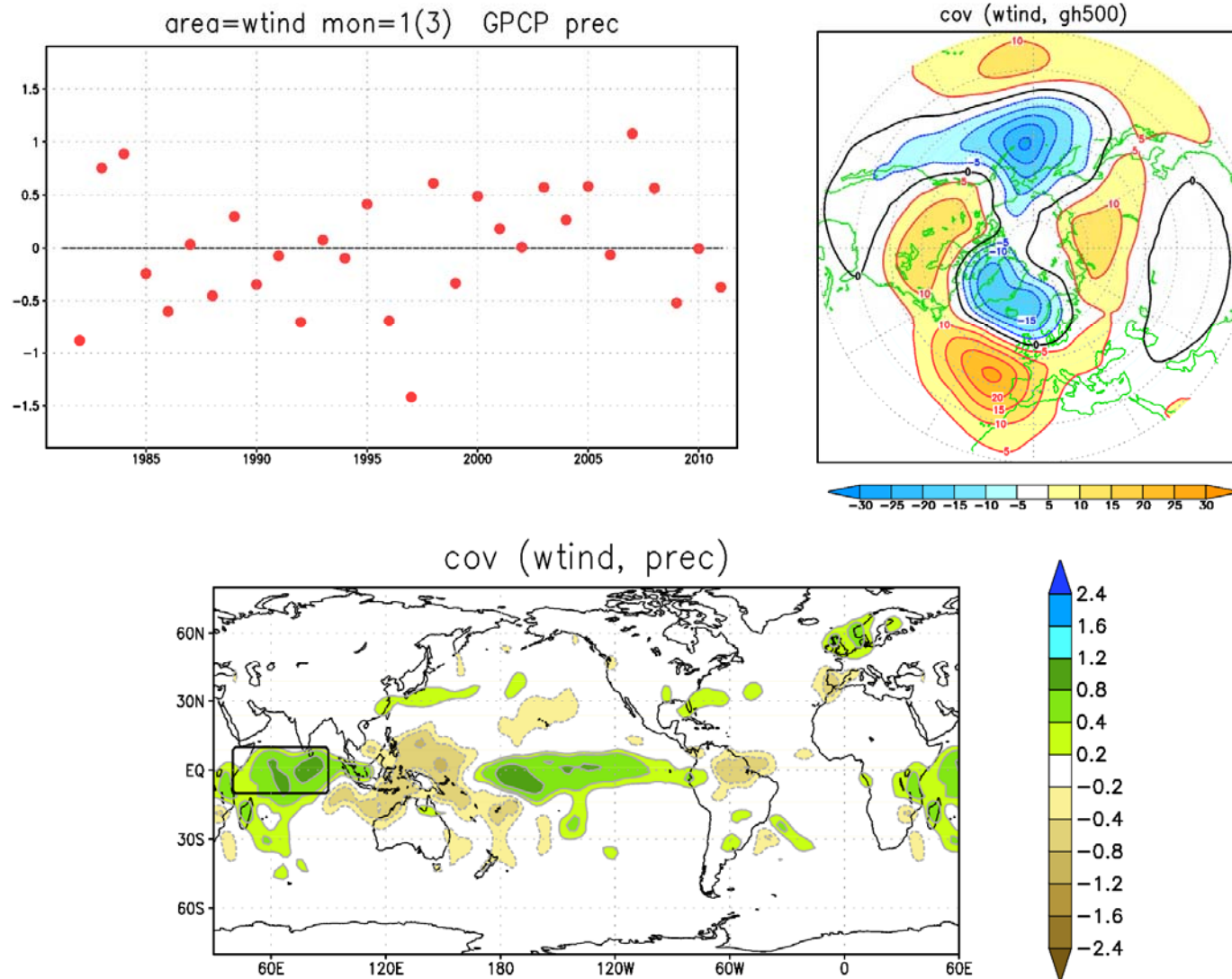
Composite in MJO  
Phase 3 + 10 days

DJF covariance with  
Indian Oc. rainfall

Inter-decadal var. in  
late 20th Century



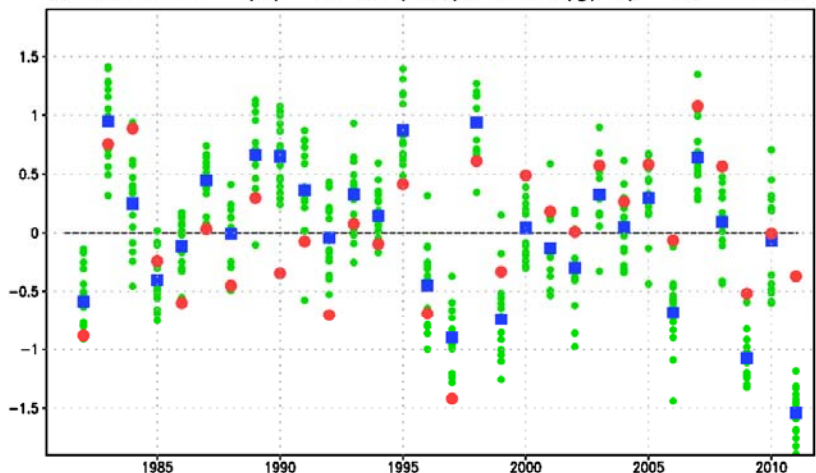
# Telecon. with DJF W Indian Oc. rainfall: GPCP2.2/ERA-int



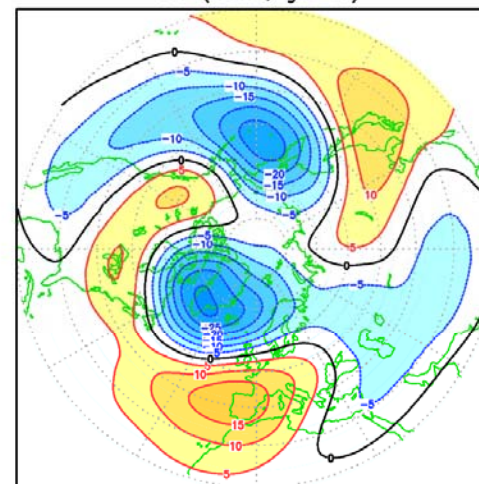


# Telecon. with DJF W Indian Oc. rainfall: Sys4, m.1

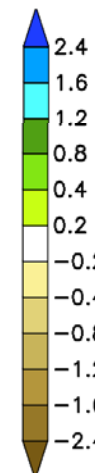
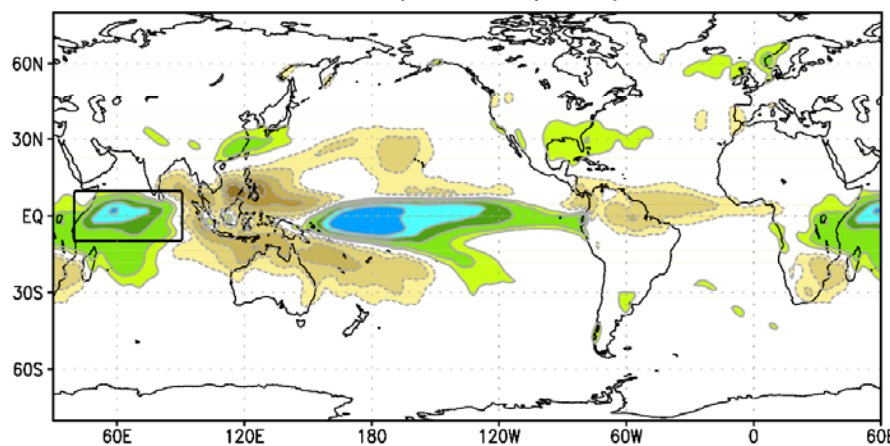
wtind mon=1(3) GPCP(red), SYS4(g/b) ac=0.660



cov (wtind, gh500)



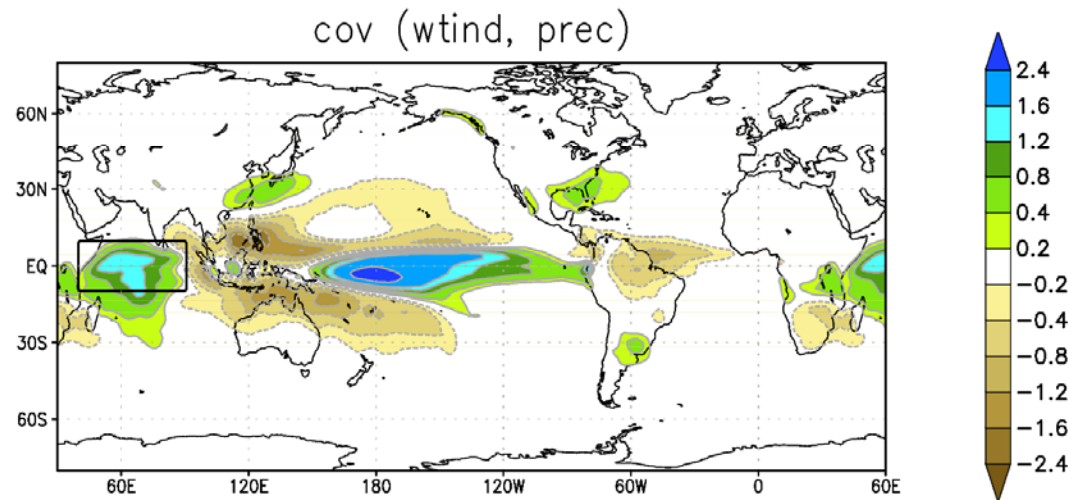
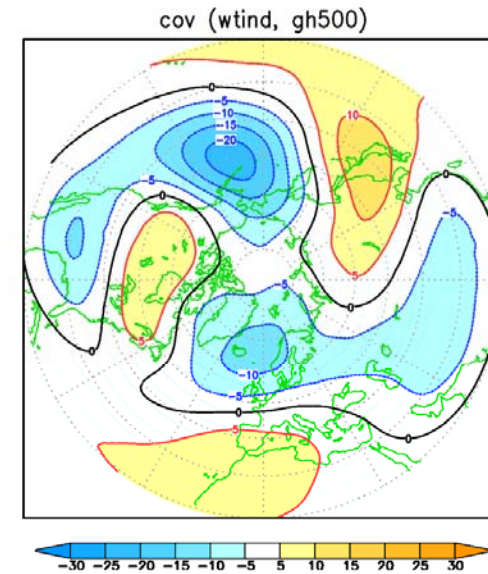
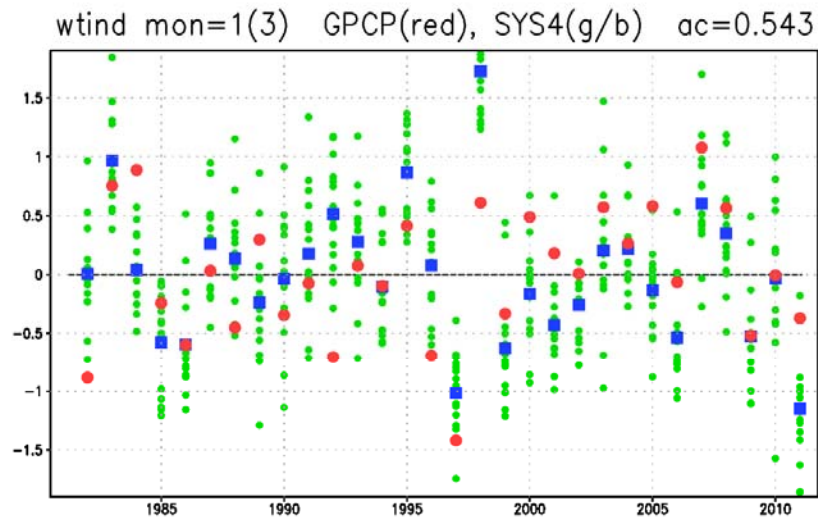
cov (wtind, prec)







# Telecon. with DJF W Indian Oc. rainfall: Sys4, m.2





# Impact on Euro-Atl. regime frequencies

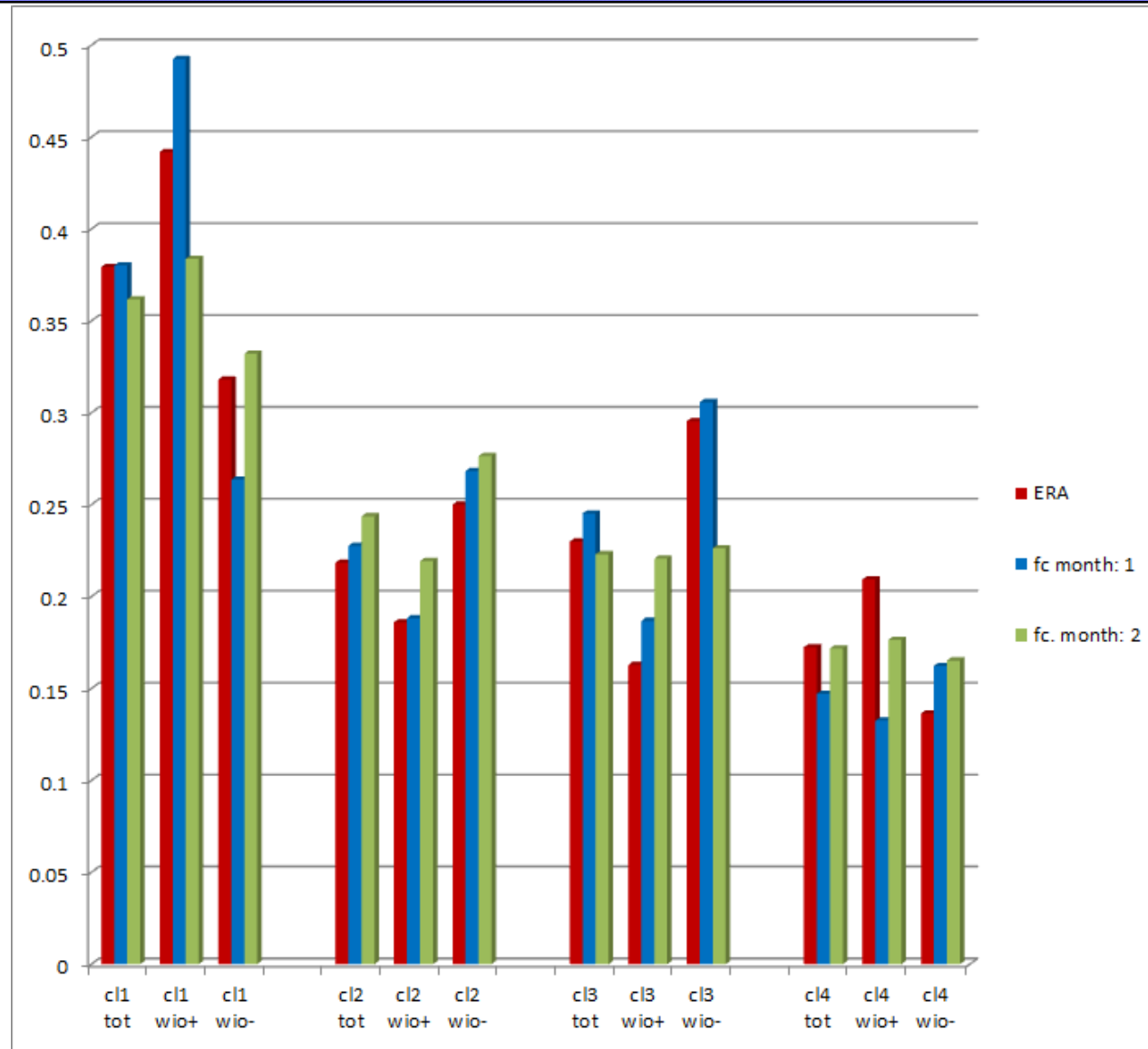
Cluster 1:  
NAO +

Cluster 2:  
Blocking

Cluster 3:  
NAO -

Cluster 4:  
Atl. ridge

*NB: clusters  
3 and 4 are  
inverted in this  
dataset*





# Conclusions

---

- Statistically significant regimes can be defined on both “hemispheric” and regional domains as clusters of 5-day mean fields in the post-1979 period.
- Regional regimes (Atlantic & Pacific) are more robust than hemispheric ones, because they can be defined in a lower-dimensional space.
- Hemispheric regimes can be interpreted as the most frequent combinations of Atlantic and Pacific regimes.
- Proper design and use of statistical significance tests is crucial for the detection of regimes in atmospheric and model datasets: significance estimation is by itself subject to uncertainties, therefore “statistical fundamentalism” should be avoided!!
- The impacts of anomalous tropical forcing on regimes are more easily detected on a regional domain. Modifications in the spatial patterns of hemispheric teleconnections/regimes can be due to differences in the strength of such impacts in the Atlantic and Pacific sectors.